Expression and intracellular processing of the 58 kDa sterol carrier protein-2/3-oxoacyl-CoA thiolase in transfected mouse L-cell fibroblasts

Barbara P. Atshaves,* Anca D. Petrescu,* Olga Starodub,† John B. Roths,† Ann B. Kier,† and Friedhelm Schroeder[1,*]

Departments of Physiology and Pharmacology,* and Pathobiology,† Texas A&M University, TVMC, College Station, TX 77843-4466

Abstract Although the sterol carrier protein 2 (SCP-2) gene encodes for two proteins, almost nothing is known of the function and potential processing of the larger transcript corresponding to the 58 kDa sterol carrier protein-2/3-oxoacyl-CoA thiolase (SCP-x), in intact cells. L-cell fibroblasts transfected with cDNA encoding for the 58 kDa SCP-x protein had a 4.5-fold increase in SCP-x mRNA transcript levels. Western blot analysis showed SCP-x protein expression reached 0.011% of total protein, representing a 4.1-fold increase over basal levels. Surprisingly, the 13.2 kDa SCP-2 protein also increased 2-fold in the transfected cells. This was consistent with part of the 58 kDa SCP-x being proteolytically processed to 13.2 kDa SCP-2 as there was no evidence of an mRNA transcript corresponding to a 13.2/15.2 kDa gene product in the transfected L-cell clones. Confocal immunofluorescence microscopy of transfected L-cells showed that SCP-x/SCP-2 co-localized in highest concentration with catalase in peroxisomes, but significant amounts appeared extra-peroxisomal. Overexpression of SCP-x significantly altered cholesterol uptake and metabolism. Uptake of exogenous [^{3}H]cholesterol and total cholesterol mass were increased 1.9- and 1.4-fold, respectively, in SCP-x expressors. Although cholesterol ester mass was unaltered, incorporation of exogenous [^{3}H]cholesterol and [^{3}H]oleic acid into cholesteryl esters increased 2.3- and 2.5-fold, respectively. These results from intact cells suggest the 13.2 kDa SCP-2 can arise from the larger SCP-2 gene product and indicate a role for the 58 kDa SCP-x protein in cholesterol uptake and intracellular cycling.—Atshaves, B. P., A. D. Petrescu, O. Starodub, J. B. Roths, A. B. Kier, and F. Schroeder. **Expression and intracellular processing of the 58 kDa sterol carrier protein-2/3-oxoacyl-CoA thiolase in transfected mouse L-cell fibroblasts.** ***J. Lipid Res.*** **1999.** 40: **610–622.**

Supplementary key words sterol carrier protein-2 • sterol carrier protein-2/3-oxoacyl-CoA thiolase • L-cell fibroblast • cholesterol trafficking

Recent advances in molecular biology have clarified several aspects of the origin of the family of proteins known as sterol carrier proteins (13.2 kDa SCP-2, 15.2 pro-SCP-2, and 58 kDa SCP-x). With the discovery that the SCP-2 gene has two initiation sites (1, 2) giving rise to two gene products (58 kDa SCP-x and 15.2 kDa pro-SCP-2) comes the challenge to determine the role(s) these proteins play in cellular cholesterol metabolism. Several issues remain to be resolved.

First, it is not known whether both the 15.2 kDa pro-SCP-2 and the 58 kDa SCP-x can be post-translationally processed to the 13.2 kDa SCP-2 protein. With rare exception (3), in most tissues the 15.2 kDa pro-SCP-2 protein is not detectable. Instead, proteolytic processing of the 15.2 kDa pro-SCP-2 protein results in cleavage of 20 N-terminus amino acids to yield the 13.2 kDa SCP-2 (4–7). In contrast, it is as yet unclear whether the larger 58 kDa protein can also give rise to the smaller 13.2 kDa or 15.2 kDa forms.

Second, it is not known whether both SCP-2 gene products physiologically function in cholesterol metabolism. Studies in vitro (8) and with transfected cells in culture suggest that the 13.2 kDa SCP-2 participates in cholesterol uptake (6, 9), intracellular transfer of sterols (7, 9, 10), cholesterol oxidation (5), and biliary secretion of sterols (11, 12). Other in vitro studies have linked the 13.2 kDa SCP-2 with the conversion of several sterol precursors to isoprenoids (13, 14) and cholesterol (15), and mitochondrial cholesterol oxidation to steroid hormones (16–19). Overexpression of the 13.2 kDa SCP-2 protein in L-cells transfected with cDNA corresponding to the 15.2 kDa pro-SCP-2 protein increased cholesteryl ester mass nearly 2-fold while triglyceride levels decreased by 60% (10). Interestingly, while SCP-2 gene ablation is expected to result in the opposite changes, this was not entirely observed. Disruption of the entire SCP-2/SCP-x gene in mice resulted in a 2-fold decrease in both liver triglyceride and cholesteryl ester mass (20). Furthermore, the knockout

Abbreviations: SCP-2, sterol carrier protein-2; SCP-x, sterol carrier protein-2/3-oxoacyl-CoA thiolase; PBS, phosphate-buffered saline; CoA, coenzyme A; GAPD, glyceraldehydephosphate dehydrogenase; L-FABP, liver fatty acid binding protein.

[1] To whom correspondence should be addressed.

mice displayed impaired catabolism of methyl-branched fatty acyl CoAs such as phytanoyl-CoA, defective thiolytic cleavage of 3-ketopristanoyl-CoA, and accumulation of high concentrations of phytanic acid when phytol-rich diets were imposed. While this would suggest that SCP-2/SCP-x may have additional important roles in peroxisomal fatty acid oxidation and/or triglyceride metabolism, two factors complicate this conclusion derived from knockout mice: *i*) both SCP-2 gene products (SCP-2 and SCP-x) were ablated concomitantly, and *ii*) compensatory changes in other proteins involved in fatty acid metabolism were observed. The liver fatty acid binding protein (L-FABP) binds phytanic acid nearly as well as normal fatty acids (13), stimulates production of phosphatidic acid, a triglyceride precursor (21), and stimulates esterification of fatty acids into specific lipid pools in favor of phospholipids rather than triglycerides in transfected cells (22). Basal levels of L-FABP in livers of the SCP-2/SCP-x knockout mice were 4-fold higher than in control mice. The fact that L-FABP normally represents 2–3% of liver cytosolic protein, as compared to 0.08% for SCP-2, suggests that the quantitative compensatory changes in L-FABP expression are substantial. Thus, while it is possible that the observed lower levels of plasma free fatty acids and liver cholesteryl esters and triglycerides in the knockout mice maybe related to decreased lipid esterification, compensatory mechanisms resulting in increased expression of related binding proteins can also be contributory.

The physiological role for 58 kDa SCP-x in cholesterol uptake, intracellular trafficking, or metabolism is not known. However, in vitro evidence shows 58 kDa SCP-x can itself transfer cholesterol between membranes (23), stimulate the conversion of 7-dehydrocholesterol to cholesterol (24), and increase sterol conversion to bile acids (25). Moreover, several studies suggest a link between SCP-2 gene products, cholesterol metabolism, and peroxisomes. Antisense SCP-2 oligonucleotide treatment of normal fibroblasts produced cells that behave like peroxisomal-deficient cells with reduced cholesterol transfer activity and decreased SCP-x levels (26). Peroxisomal-deficient cells show a 75% decrease in cholesterol biosynthesis, reduced cellular levels of SCP-2, and impaired LDL cholesterol processing (27–29). Also, the 13.2 kDa SCP-2 protein binds several cholesterol intermediates including geranyl-PP, farnesyl-PP, and dimethylallyl-PP (13) and stimulates the enzyme isopentyl transferase (14). Finally, it has been shown that cholesterol synthesis from mevalonate to farnesyl pyrophosphate occurs in peroxisomes and that peroxisomes can convert mevalonate to cholesterol in vitro (28, 30, 31).

To further elucidate the cellular role of sterol carrier proteins, L-cell fibroblasts were transfected with cDNA encoding for the 58 kDa sterol carrier protein SCP-2/3-oxoacyl-CoA thiolase, i.e., SCP-x. Expression of both SCP-x and SCP-2 were increased in the transfected clones which suggests that the expressed 58 kDa SCP-x protein was partially processed in the intact cells to yield 13.2 kDa SCP-2. Immunofluorescence imaging showed that SCP-2/SCP-x colocalized with catalase with some extraperoxisomal staining also observed. Increased expression of the 58 kDa SCP-x and, concomitantly, its cleavage product 13.2 kDa SCP-2, enhanced incorporation and esterification of cholesterol as well as intracellular cycling of these lipids.

MATERIALS AND METHODS

Materials sources

Silica gel G plates were purchased from Analtech (Newark, DE); petroleum ether, diethyl ether, acetic acid, and methanol were from Fisher (Pittsburgh, PA); penicillin, streptomycin, and trypsin-EDTA were purchased from Sigma Chemical Company (St. Louis, MO); lipid standards were purchased from Steraloids (Wilton, NH); [^{3}H]cholesterol and [^{3}H]oleic acid were purchased from DuPont New England Nuclear (Boston, MA); and TRIzol reagent, Prestain protein molecular weight standards, and G418 were purchased from Gibco BRL (Life Technologies, Gaithersburg, MD). All reagents and solvents used were of the highest grade available and were cell culture tested as necessary.

L-cell culture

Control and transfected murine L-cells (L arpt$^-$tk$^-$) were grown to confluency in Higuchi medium (32) supplemented with 10% fetal bovine serum (Hyclone, Logan, UT) as stated in the text (6, 33). Transfected cells were initially grown on selection in media containing G418 at a concentration of 700 μg/ml active drug and thereafter in media without G418.

Construction of 58 kDa SCP-x expression vector and transfection into L-cells

Development of cell lines transfected with cDNA encoding for the 15.2 kDa pro-SCP-2 protein was described earlier (6). The entire coding region of mouse 58 kDa SCP-x cDNA was cloned into the eukaryotic expression vector pcdef3, a generous gift from Dr. Jerome Langer (Rutgers University, Piscataway, NJ). The cDNA was generated using the 1st-strand™ cDNA Synthesis Kit from Clontech (Palo Alto, CA) with total RNA being prepared according to standard protocols (34). The 1st-strand cDNA encoding for SCP-x was amplified using the *Pfu* DNA polymerase from Stratagene (La Jolla, CA) under conditions optimized for high fidelity DNA synthesis using primers designed with the following restriction enzyme sites: *Eco*RI in the 5′ end and *Xba*I at the 3′ end for easy ligation into pcdef3 (35). DNA sequencing was performed to verify identity and fidelity. The cDNA (1641 base pairs) was cloned downstream from the human polypeptide chain elongation factor 1α (EF-1α) promoter and upstream from the bovine growth hormone (BGH) polyadenylation and splice sequences. The plasmid containing the correct size insert was designated pBA35-X. To prepare for transfection, plasmid pBA35-x and the vector pcdef3 were isolated on a large scale with Qiagen Maxi-prep columns (Qiagen, Inc., Chatworth, CA). Two different transfection methods were tested for production of stable transfection products, the standard calcium phosphate method for clone 58-1 and LipofectAMINE reagent (Gibco BRL, Life Technologies, Gaithersburg, MD) for clone 58-2, with mock transfectants (clones transfected with vector DNA without cDNA insert) isolated from both methods. Approximately 1–2 μg of DNA was used per transfection experiment with procedures followed as described in the product literature. Twenty-four hours after transfection, the cultures were placed on selection medium containing 700 μg/ml G418. Resistant clones were selected after 10–11 days using clonal tubes. Several clones arising from transfection with the expression construct and the vector without cDNA were expanded from 24-well dishes to 6-well dishes and then 10-cm plates for further analysis.

Northern blot analysis

Total RNA from mouse liver, L-cells, and transfected L-cell clones was isolated using TRIzol Reagent (Gibco BRL, Life Technologies, Gaithersburg, MD) according to product literature. The RNA samples (20 μg) were electrophoresed at 90 volts for 4 h in 1% agarose gel prepared in MOPS buffer (40 mm morpholinopropanesulfonic acid, 10 mm sodium acetate, 10 mm EDTA, pH 7.2) containing 0.66% formaldehyde (36). The RNA was transferred by capillary action to positively charged nylon membranes (Boehringer Mannheim, Indianapolis, IN). Radioactive probes were prepared by random priming method (37) using High Prime kit from Boehringer Mannheim and ^{32}P-dCTP (3000 Ci/mmol, NEN Life Science Products, Inc, Boston, MA). A *Bam*HI/*Xba*I fragment from SCP-2 cDNA (0.55 kb) was used to probe for SCP-2 and SCP-x mRNAs. Mouse glyceraldehydephosphate dehydrogenase (GAPD) mRNA was used as a positive control for the prepared RNA.

Protein purification

Recombinant human SCP-2 and pro-SCP-2 proteins were purified as described (38). Recombinant mouse 58 kDa SCP-x was purified from an expression construct made to produce protein for standards and antibody production. The cDNA was generated by RT-PCR following product literature (1st-strand™ cDNA Synthesis Kit from Clontech, Palo Alto, CA) using the *Pfu* DNA polymerase from Stratagene (La Jolla, CA). Primers were designed with unique restriction sites (*Xho*I and *Bgl*II) for easy cloning into the expression vector pET15b (Novagen, Madison, WI) with sequencing performed to ensure fidelity and identity of product. By cloning the cDNA into the pET vector, an N-terminal HisTag was attached to the SCP-x protein which allowed for easy purification using affinity chromatography as described below. The resulting plasmid (pBA34-X) was transformed into the *Escherichia coli* host strain BL21(DE3)pLysS and protein expression was determined. Several colonies were screened for expression before expanding to large scale protein production. Overnight cultures of *E. coli* cells expressing SCP-x were used to inoculate 4 liters of Luria Broth (LB) with 100 μg/ml ampicillin and 35 μg/ml chloramphenicol. The cultures, grown at room temperature, were induced with lactose (0.4 mm) at OD_{595} = 0.6 and harvested after 3 h growth to reduce formation of inclusion bodies. The 4 liters of culture were then centrifuged at 4000 *g* for 10 min at 8°C with the resulting pellet stored at −70°C up to 1 month or used directly. The pellet was resuspended in 60 ml buffer A (50 mm phosphate, 500 mm NaCl, 10% glycerol, 10 mm β-mercaptoethanol, 50 mm imidazol, 1 μm leupeptin, 2 μm pepstatin, and 100 μg/ml phenylmethylsulfonyl fluoride, pH 7.0), sonicated in pulse mode six times for 1 min at 8°C, and then centrifuged at 14,000 *g* for 30 min at 8°C. Under the above growth conditions, up to 60% of the total protein remained soluble and was further purified by affinity chromatography using NiNTA (nickel nitrilo-tri-acetic acid) resin (3 ml) from Qiagen (Qiagen, Inc., Chatsworth, CA) where, after loading the supernatant, the resin was washed with buffer B (buffer A at pH 6.0) until an OD_{280} <0.05 was reached, followed by elution of proteins with a linear gradient (0–1.2 m imadazole in buffer B, 80 ml total volume). Several slight contaminants were removed in the next step using a gel filtration resin (Sephadex G-100, Pharmacia, Piscataway, NJ) equilibrated in buffer C (50 mm KH_2PO_4, 100 mm NaCl, 10% glycerol, 0.5 mm DTT, pH 6.5). The HisTag was then removed from the protein using thrombin (Pharmacia, Piscataway, NJ) after the protein was exchanged into buffer D (buffer C without the DTT, pH 7.1). In the last step, an anion exchange resin was used (Q-Sepharose fast flow, Pharmacia, Piscataway, NJ) equilibrated in buffer E (50 mm KH_2PO_4, 100 mm NaCl, 20% glycerol, 1 mm DTT, pH 8.0) where the protein was eluted by linear gradient (0–1 m NaCl in buffer E, 1 liter total volume). Alternatively, a cation exchange resin (CM fast flow from Pharmacia, Piscataway, NJ) was used equilibrated in buffer F (20 mm MES, 20% glycerol, pH 6.5) and eluted by a linear gradient of 0–1 m NaCl in buffer F, 1 liter total volume. Approximately 2–3 mg of protein per liter of culture with purity of 98% or better was isolated in this manner. Protein samples were run on tricine gels (10%) and stained with Coomassie blue dye (0.6 g Coomassie Brilliant Blue G-250, 0.1 g SDS, 0.25 g Tris-HCl, and 1.5 g glycine brought up in 500 ml of 50% trichloroacetic acid), followed by destaining in 7% glacial acetic acid to show the results of each purification step.

Antibody production for Western blotting

The experimental protocols for the use of laboratory animals were approved by the appropriate institutional review committee and met AAALAC guidelines. Female NZW rabbits (2 kg) were purchased from Hazleton Research Products (Denver, PA) and were injected with purified mouse recombinant 58 kDa protein and Freund's adjuvant as described (39) to produce polyclonal anti-58 kDa SCP-x antisera. The anti-SCP-x antibody was purified by affinity chromatography by coupling 58 kDa SCP-x protein to CNBr-Sepharose 4B (Pharmacia Biotech, Uppsala, Sweden) using the procedure recommended by the manufacturer. At this stage, the antibody was used for Western blotting. Because all the SCP-2 gene products share the same 13.2 kDa C-terminus, the antisera showed cross-reactivity with 13.2 kDa SCP-2, 15.2 kDa pro-SCP-2, and 58 kDa SCP-x proteins, along with a cross-reactive band at 30 kDa which was recently shown to be a protein outside the SCP-2 family (40) (see Results).

Affinity purification of antibodies for immunocytochemistry

For immunocytochemistry experiments, additional purification of the anti-SCP-x antisera was necessary. Therefore, the polyclonal antibody was further purified by incubating the rabbit anti-SCP-x serum with mouse liver homogenate that had been run on large-scale Tricine-PAGE gels from which the 58 kDa SCP-x, 13.2 kDa SCP-2, and 15.2 kDa pro-SCP-2 proteins had been excised. The non-adsorbed antisera were removed by sedimentation of the gel and the supernatant containing anti-SCP-x was retained. The resultant antibody showed no cross-reactivity to the 30 kDa protein and was used for immunocytochemistry experiments.

Western blotting

The expression of SCP-x in L-cell clones transfected with plasmid pBA35-X was determined by quantitative Western blotting. Cells were washed in phosphate-buffered saline, trypsinized, and centrifuged. The cell pellets were resuspended in lysing buffer (10 mm Tris-HCl, 100 mm NaCl, 1 μm leupeptin, 2 μm pepstatin, and 100 μg/ml phenylmethylsulfonyl fluoride, pH 7.0) and sonicated in pulse mode four times for 20 sec over 30 min at 4°C. The samples were centrifuged at 10,000 *g* for 20 min at 4°C. Exact protein concentrations of the resulting supernatants were determined by the Bradford method (41). Protein samples (50 μg of homogenate) were run on tricine gels (16%). The protein was transferred to 0.45 μm nitrocellulose paper (Sigma Chemical Co., St. Louis, MO) by electroblotting in a continuous buffer system at 0.8 mA/cm^2 for 3 h. After transfer, the blot was blocked in 3% gelatin for 30 min, washed three times in TBST (10 mm Tris [pH 8.0], 150 mm NaCl, 0.05% Tween 20) for a total of 15 min, then incubated overnight in affinity-purified polyclonal rabbit anti-SCP-X antisera (1:1000 dilution) in 1% gelatin in TBS (10 mm Tris [pH 8.0], 150 mm NaCl). This polyclonal was also immunoreactive to the 13.2 kDa and 15.2 kDa proteins and was successfully used to detect SCP-x and SCP-2 expression in the protein samples. The blot was rinsed two times in TBST, followed by two

washes of TBS, and then incubated with affinity-isolated goat anti-rabbit IgG (whole molecule) alkaline phosphatase conjugate Sigma Chemical Co. The blot was washed two times with TBST followed by two washes of TBS, once in alkaline phosphatase (AP) buffer (100 mm Tris [pH 9.0], 100 mm NaCl, 5 mm $MgCl_2$), and then developed with Sigma Fast 5-bromo-4-chloro-3-indolyl phosphate/nitro blue tetrazolium tablets (Sigma Chemical Company). Some blots were processed with the Phototope-HRP Western blot detection kit (New England Biolabs, Inc., Beverly, MA). Details were as described in the product literature. Proteins and RNA were quantitated by densitometric analysis after image acquisition using a single-chip CCD (charge coupled device) video camera and a computer workstation (IS-500 system from Alpha Innotech, San Leandro, CA). Image files were analyzed (mean 8-bit grey scale density) on Power Macintosh workstation using NIH Image, a program written by W. Rasband and available by anonymous FTP from zippy.nimh.nih.gov.

Immunofluorescence microscopy on transfected cell lines

Indirect immunolabeling of expression clones was performed on cells grown to confluence on glass coverslips using polyclonal antibody that cross-reacted with all SCP-2 gene products. The cells were fixed and permeabilized using cold methanol followed by rehydration with borate buffer (57 mm, pH 8.2). After blocking with 2% ovalbumin in PBS, the cells were incubated with rabbit anti-mouse SCP-2 (1:20 dilution) for the single label experiments, and a mixture of the anti-mouse SCP-2 antibody and an immunoglobulin (IgG) fraction of sheep antiserum to bovine liver catalase (BioDesign, Kennebunk, ME) at a 1:40 and 1:20 dilution, respectively for double-label indirect immunofluorescence. Both antibodies were titered at a series of dilutions and in all cases the pattern of staining remained the same. The cells were washed with PBS, and, for the single label experiments, fluorescein conjugate of goat anti-rabbit IgG (Sigma Chemical Co.) at a 1:100 dilution was applied to the coverslips. For the double-label indirect immunofluorescence, a mixture of secondary reagents consisting of Texas Red conjugate of goat anti-rabbit IgG (H + L chain specific) antibody (Southern Biotechnology Assoc., Birmingham, AL) and fluorescein conjugate of donkey anti-sheep IgG (Sigma Chemical Co.) at a 1:50 dilution was added. For the single and double-label experiments, the incubations were performed at 37°C for 30 min in a humid chamber. The cells were washed extensively and the coverslips were mounted on slides with Slow-Fade medium (Molecular Probes, Eugene, OR). Immunostained cell preparations were examined either by conventional epifluorescence microscopy, using an Olympus Vanox AHGS3 research photomicroscope equipped with a 100W Mercury fluorescence illuminator, or by confocal microscopy using a Bio-Rad (Hercules, CA) MRC-1024 Laser Scanning Confocal Imaging system. On the Vanox, digital images were acquired using a Peltier-cooled 3-chip CCD camera system (model DEI-750) from Optronics Corporation (Goleta, CA) coupled with a 24-bit RGB Neotech frame grabber (Graftek Imaging, Austin, TX) in a Power Macintosh 8100 computer (Apple Corp., Cupertino, CA). On the Bio-Rad MRC-1024 confocal images were acquired using 1 to 3 photomultiplier tubes (PMTs) under the control of LaserSharp v.3.1 software (Bio-Rad). The MRC-1024 system had a 15 mW krypton–argon laser (American Laser Corp., Salt Lake City, UT) with a 5 mW output measured at the microscope stage, and a Zeiss Axiovert 135 inverted epifluorescence microscope (Zeiss, Thornwood, NY) using a 63× oil immersion objective with a numerical aperture of 1.4. Photobleaching was minimized by exposing samples to the light source for minimal time periods. Fluorescence imaging was performed using 488 nm excitation and a OG515 long path filter for FITC (green channel) and 568 nm excitation with a 680/32 band path emission filter for Texas Red (red channel). For co-localization experiments, the confocal images derived from the red and green channels were combined and appeared as yellow to orange where superimposition occurred.

Labeling of cells with [^{3}H]cholesterol or [^{3}H]oleic acid

L-cell control, mock-transfected, and transfected cell lines were cultured in 10-cm dishes in Higuchi medium containing 10% fetal bovine serum and [^{3}H]cholesterol (0.1 μCi/ml medium) for 1, 3, 6, 9, 15, 20, and 25 h at 37°C. The radiolabeled medium was added after a phosphate-buffered saline (PBS) prewash was performed to remove non-adherent cells. At the indicated time intervals, the medium was removed quickly, the cells were washed with PBS, frozen on liquid N_2, and scraped into n-hexane–2-propanol extraction solvent 3:2 (v/v) (42, 43). The samples were then analyzed for lipid content as described below. The procedure for [^{3}H]oleic acid incorporation into the cells was basically the same as for [^{3}H]cholesterol with the following exceptions: cells were incubated at 37°C for 60 min with 2 μm oleic acid containing 1.0 μCi of [^{3}H]oleic acid with a final specific activity of 0.1 μCi/nmol.

Lipid analysis of cells

After extracting the radiolabeled samples as above, the protein portion was pelleted by centrifugation at 1,400 rpm for 20 min using a IEC PR-6000 centrifuge (International Equipment, Needham Heights, MA). The supernatant was separated, evaporated to dryness under a stream of nitrogen, and then brought up in chloroform (200 μl). The lipid classes were resolved using Silica gel G thin-layer chromatography plates (Analtech, Newark, DE) developed in the following solvent system: petroleum ether–diethyl ether–methanol–acetic acid 90:7:2:0.5 (44). Bands were visualized by exposing the plates to iodine and compared to commercially prepared controls of cholesterol, cholesteryl ester, triglycerides, phospholipids, and fatty acids (Steraloids, Wilton, NH). Radiolabeled lipids were quantified in liquid scintillation cocktail (Scinti Verse, Fisher Scientific, Pittsburg, PA) on a Packard 1600TR liquid scintillation counter (Meridian, CT). The protein pellets were air-dried, resuspended in 0.2 N KOH, and heated overnight at 65°C before being quantified for protein content.

Lipid determination

All glassware was washed with sulfuric acid/chromate before use. Cells isolated from two 10-cm plates were considered n = 1. Cholesterol, cholesteryl ester, and triglyceride content were determined by the method of Marzo et al. (44). Protein concentrations were determined by the method of Bradford (41). The lipids were separated using the solvent system and procedure as described above.

Statistics

All values were expressed as the mean ± SEM with n and *P* indicated in the Results section. Statistical analyses were performed using Student's *t*-test (GraphPad Prism, San Diego, CA). Values with $P < 0.05$ were considered statistically significant.

RESULTS

Vector preparation and L-cell transfection

Mouse L-cells were stably transfected with cDNA encoding sterol carrier protein-2/3-oxoacyl-CoA thiolase (SCP-x) to produce clones expressing the 58 kDa SCP-x protein. The 1641 bp mouse cDNA encoding for SCP-x was generated by reverse transcription polymerase chain reaction (RT-PCR) with primers designed to include *Eco*RI and

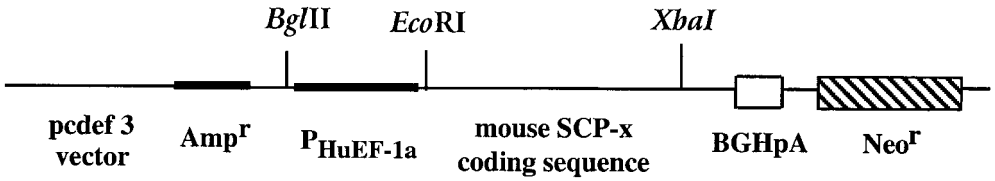

Fig. 1. Linear map of plasmid pBA35-X. The entire coding region of mouse 58 kDa SCP-x cDNA was cloned into the unique *Eco*RI / *Xba*I restriction sites of vector pcdef3 between the human polypeptide chain elongation factor 1α ($P_{HuEF\text{-}1\alpha}$) promoter and bovine growth hormone (BGHpA) polyadenylation and splice sequences. Amp, ampicillin resistance gene. Neo, neomycin cassette.

*Xba*I endonuclease restriction sites for easy cloning into the pcdef3 vector. The resulting plasmid was designated pBA35-X (**Fig. 1**). After transfection and selection in G418, several stable cell lines survived and were expanded for further analysis.

Northern analysis on transfected clones

Northern blot analysis was performed (**Fig. 2**) to verify transcription of the cDNA encoding for 58 kDa SCP-x and, to rule out the possibility that the construct could generate a mRNA transcript corresponding to the 46 kDa (N-terminal thiolase portion of SCP-x), 15.2 pro-SCP-2, or 13.2 SCP-2 proteins. Multiple transcripts were observed (derived from alternative polyadenylation sites). The two larger transcripts (3.0 and 2.2 kb) corresponded to the SCP-x mRNA while the two smaller messages (1.6 and 0.9 kb) were associated with the 15.2 kDa pro-SCP-2 mRNA (5, 45–47). In the mouse liver sample (Fig. 2, lane 1), all four transcripts were present when the blot was probed with cDNA encoding for the 15.2 kDa protein. Lanes 2, 3, and 4 were loaded with RNA isolated from L-cells, 58 kDa expressors, and 15.2 kDa pro-SCP-2 expressors, respectively. While both the untransfected L-cell control (lane 2) and 58 kDa SCP-x expression clone (lane 3) showed evidence of the 2.2 kb and, to some extent, the 0.9 kb band, the 58 kDa SCP-x expressor showed a 4.5-fold increase in the 2.2 kb mRNA transcript. Interestingly, the 3.0 kb message was not observed. As expected, the 15.2 kDa pro-SCP-2 expressor, loaded as a control (lane 4), showed increased production of the 1.6 kb transcript (15-fold). No evidence was found indicating the presence of mRNA that could produce increased levels of any other protein in the SCP-2 family. The smaller panels below the main blots show the mRNA encoding for mouse glyceraldehydephosphate dehydrogenase (GAPD) which served as a positive control for all the RNA prepared.

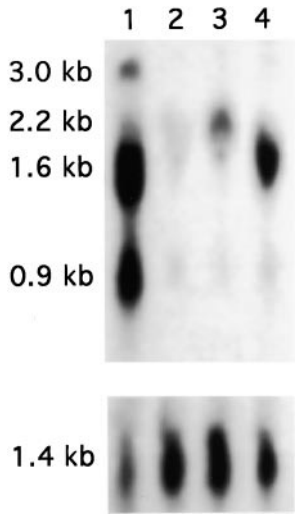

Fig. 2. Northern blot analysis on control and expression clones. The blot was loaded with total RNA (20 μg) from the following sources: lane 1, mouse liver; lane 2, untransfected L-cells; lane 3, 58 kDa SCP-x expression clone; and lane 4, 15 kDa pro-SCP-2 expression clone. The blot was probed with cDNA corresponding to the 15.2 kDa pro-SCP-2 protein. The smaller panels below the main blots show mRNA encoding for mouse glyceraldehydephosphate dehydrogenase (GAPD) and serve as an internal control for all the RNA prepared.

SCP-x expression in transfected L-cells

To examine the expression of 58 kDa SCP-x in transfected L-cells by Western blotting, it was first necessary to purify the recombinant 58 kDa SCP-x protein to generate polyclonal anti-SCP-x antisera. Mouse recombinant 58 kDa SCP-x protein was subcloned and purified as described in the Methods section. The purification level at several key steps is shown in **Fig. 3** with the final product reaching 98% or better purity.

Several transfected clones revealed increased SCP-x protein expression as seen in **Fig. 4** and **Table 1**. The level of SCP-x expression was quantitated by densitometric

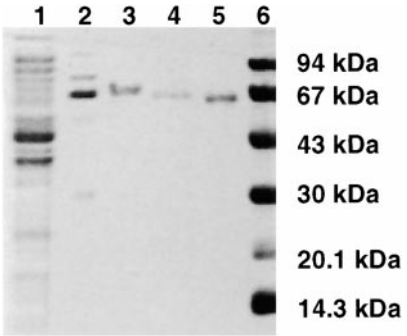

Fig. 3. Recombinant 58 kDa SCP-x protein purification. A tricine gel (10%) was loaded as follows: lane 1, supernatant after sonication; lane 2, sample after NiNTA column; lane 3, sample after G-100 column; lane 4, sample after HisTag is removed; lane 5, sample after Q-Sepharose column; and lane 6, molecular weight standards.

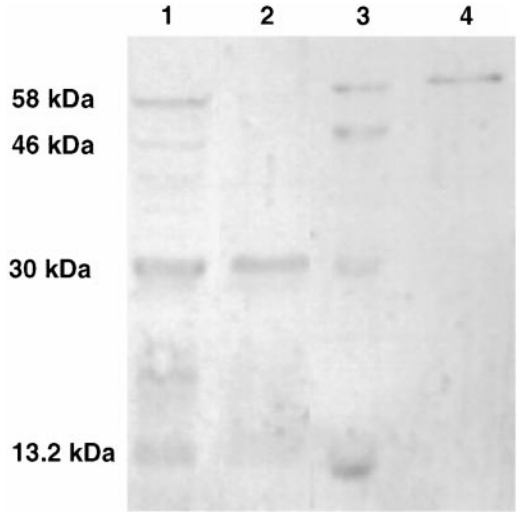

Fig. 4. Western blot showing L-cells expressing 58 kDa SCP-x/13.2 kDa SCP-2 proteins. Cell homogenates were run on a 16% Tricine gel, loaded as follows: lane 1, transfected L-cell clone 58-1 (50 μg); lane 2, untransfected L-cell homogenate (50 μg); lane 3, rat liver homogenate (10 μg); and lane 4, mouse recombinant 58 kDa SCP-x protein (7 ng). The blot was probed with affinity-purified polyclonal anti-SCP-x as described under Methods.

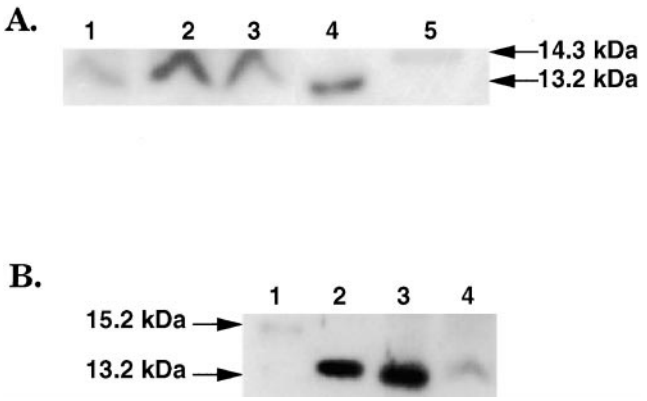

Fig. 5. Panel A: Western blot analysis of SCP-x expression clones showing expression of 13.2 kDa SCP-2 protein. Cell homogenates were run on a 16% Tricine gel, loaded as follows: lane 1, untransfected L-cell homogenate (50 μg); lane 2, transfected L-cell clone 58-2 homogenate (50 μg); lane 3, transfected L-cell clone 58-1 homogenate (50 μg); lane 4, human 13.2 kDa SCP-2 protein standard (12 ng); lane 5, 14.3 kDa molecular weight marker (lysozyme protein). Panel B: Western blot analysis of 13.2 and 15.3 kDa SCP-2 protein standards and cell homogenates. The 16% Tricine gel was loaded as follows: lane 1, 15.2 kDa pro-SCP-2 protein standard (1 ng); lane 2, 13.2 kDa SCP-2 protein standard (5 ng); lane 3, rat liver homogenate (8 μg); and lane 4, transfected L-cell clone 58-1 (50 μg). The blots were probed with affinity-purified polyclonal anti-SCP-x as described in Methods.

analysis of the Western blots and calibrated by comparison to known quantities of recombinant 58 kDa SCP-x (see Methods) with clones 58-1 and 58-2 showing the highest expression at 0.011% ± 0.0015 (n = 3) and 0.009% ± 0.0017 (n = 3) respectively, of total protein. This represented a 4.1-fold increase over basal levels (Table 1). As the polyclonal antibody used to probe the Western blot was derived from the entire 58 kDa recombinant protein, it was able to recognize the 58, 46, and 13.2 kDa protein products. There was no detectable 15.2 kDa pro-SCP-2 in either the control cells or expression clones. Clone 58-1 (Fig. 4, lane 1) showed the presence of all 3 (58, 46, and 13.2 kDa) SCP-2 gene products. A reactive protein at 30 kDa, also present in the L-cell and rat liver controls, was recently shown not to be a SCP-2 gene product (40).

To determine whether the expressed 58 kDa SCP-x in the transfected clones may have been proteolytically processed to 13.2 kDa SCP-2, additional Western blotting was performed (**Fig. 5**). An anti-SCP-2 immunoreactive protein band running with the 13.2 kDa SCP-2 standard showed increased expression in transfected clones (Fig. 5, panel A). This immunoreactive anti-SCP-2 band was not the 15.2 kDa pro-SCP-2, as shown in a separate Western blot run with the 15.2 kDa pro-SCP-2 standard (Fig. 5, panel B). Clearly, the low molecular weight protein from the transfected L-cells and liver samples was the 13.2 kDa SCP-2. Quantitative analysis (Table 1) revealed a 2-fold increase in 13.2 kDa SCP-2 protein expression (0.015% ± 0.0014 total protein in both transfected clones, $P < 0.009$, n = 6) over control L-cells (0.008% ± 0.0014 total protein). If the 58 kDa SCP-x is cleaved to yield a 13.2 kDa SCP-2 band, then another expected fragment of this cleavage should appear near 46 kDa. Indeed, the expected cleavage product near 46 kDa is detectable in transfected cells (Fig. 4, lane 1) and in liver (Fig. 4, lane 3) but is absent in control L-cells (Fig. 4, lane 2). However, the intensity of the 46 kDa band in the 58 kDa SCP-x expressors was insufficient for accurate quantitation, probably due to the relative affinity of the polyclonal antibodies for the two peptides (13.2 versus 46 kDa). Thus, the appearance of increased 13.2 kDa SCP-2 and the 46 kDa protein is consistent with the 58 kDa SCP-x protein being proteolytically cleaved.

In summary, data from Western and Northern blot analysis show that transfected L-cell expression clones had increased levels of mRNA transcripts corresponding to the 58 kDa SCP-x protein. As no concurrent increased production of the mRNA transcript associated with the 15.2 kDa pro-SCP-2 protein was detected, the altered 13.2 kDa expression levels observed in Western blots were most likely due to 58 kDa SCP-x being proteolytically processed to 13.2 kDa SCP-2. The proteolytic site in the 58 kDa SCP-x appears similar to that observed for the 15.2 kDa pro-

TABLE 1. Quantitation of 58 kDa SCP-x and 13.2 kDa SCP-2 protein expression in control and 58 kDa SCP-x expression clones

Protein	Control	Clone 58-1	Clone 58-2
		% total protein	
58 kDa SCP-x	0.0027 ± 0.0006	0.011 ± 0.0015[a]	0.009 ± 0.0017[a]
13.2 kDa SCP-2	0.008 ± 0.0014	0.015 ± 0.0014[b]	0.015 ± 0.0013[b]

Values were determined from Western blot analysis and represent means ± SEM (n = 6 for 13.2 kDa SCP-2 and n = 3 for 58 kDa SCP-x quantitation in transfected clones).

[a] $P < 0.02$; [b] $P < 0.005$; indicate significance as compared to control.

SCP-2 in liver and in transfected L-cells overexpressing the 15.2 kDa pro-SCP-2 (6). In both cases the 13.2 kDa SCP-2, but not the 15.2 kDa pro-SCP-2, was detected on Western blotting.

Immunocytochemistry of transfected L-cells

In liver, anti-SCP-2 immunoreactive proteins are found in highest concentration in peroxisomes (48–50). However, it is not clear whether the SCP-2 expressed in transfected L-cells is likewise appropriately targeted. To first establish the pattern of immunolabeling for 58 kDa SCP-x and 15.2 kDa pro-SCP-2 expressors, L-cells transfected with cDNA encoding for 58 kDa SCP-x (**Fig. 6**, panel A), 15.2 kDa pro-SCP-2 (Fig. 6, panel B), and no cDNA (Fig. 6, panel C) were indirectly immunolabeled with affinity-purified polyclonal rabbit anti-mouse SCP-x antibody followed by FITC-conjugated goat anti-rabbit IgG. A punctate pattern was revealed for both the 58 kDa SCP-x and 15.2 kDa pro-SCP-2 expressors, while very little fluorescence was detected in the untransfected (Fig. 6, panel C) or mock transfected (not shown) control L-cells. Thus, the punctate pattern of both SCP-2 gene products was very similar.

In order to determine whether the punctate pattern in the 58 kDa SCP-x expressors was due to localization in peroxisomes, the cells were simultaneously immunolabeled with affinity-purified antisera to SCP-x and a peroxisomal marker, catalase. This was done by immunolabeling for SCP-x with Texas Red-conjugated goat anti-rabbit IgG (**Fig. 7**, panel A) and catalase with FITC-conjugated donkey anti-sheep IgG (Fig. 7, panel B). Both antibodies showed a punctate pattern. To determine the degree of co-localization of the two proteins, the two images were superimposed (Fig. 7, panel C). Clearly, in many of the punctate fluorescing particles, the antisera co-localized the SCP-x and catalase in the same organelle, i.e., peroxisomes, as shown by the yellow to orange color. This type of visual qualitative evaluation can be put into graphic form as a pixel fluorogram (51) as seen in Fig. 7, panel D where the correlation between the two immunolabeled organelles is shown. If all of the SCP-x and catalase had co-localized completely then the fluorogram would have shown yellow points only along the diagonal and the correlation coefficients would have equaled 1. While a significant population of data points does fall on this line, the pixel fluorogram (panel D) and superimposed image (panel C) shows an additional population of red (SCP-x) stained as well as green (catalase)-stained organelles. In addition, the correlation coefficients are 0.47 and 0.6, respectively. These results show that anti-SCP-x immunoreactivity is co-localized with anti-catalase to peroxisomes but also includes significant extraperoxisomal staining.

Incorporation of [^{3}H]cholesterol into the free cholesterol pool of transfected L-cells

While the 58 kDa SCP-x protein was shown to enhance intermembrane sterol movement in vitro (23–25), it was important to examine whether this occurred in the transfected L-cells. Internalization and entry of exogenous cholesterol into the cellular free cholesterol pool was deter-

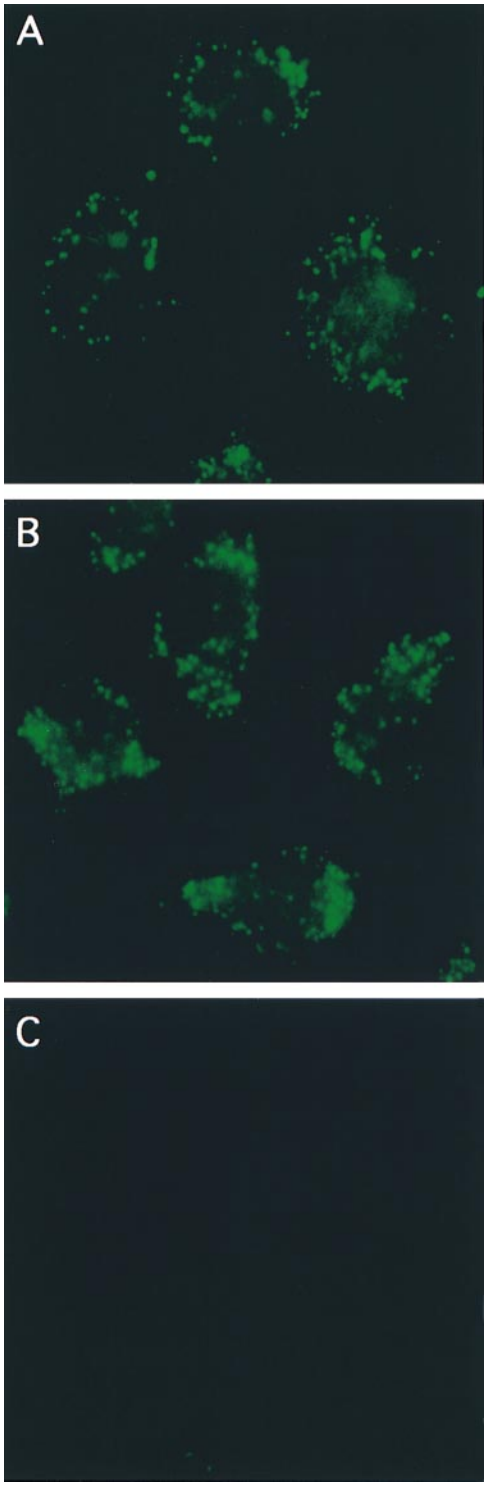

Fig. 6. Indirect immunolabeling of transfected L-cells. 58 kDa SCP-x expressor (panel A), 15.2 kDa pro-SCP-2 expressor (panel B), and untransfected L-cells (panel C) were indirectly immunolabeled with polyclonal rabbit anti-mouse SCP-2 antibody followed by FITC-conjugated goat anti-rabbit IgG as described in Methods. A punctate pattern was revealed for all cell lines, considerably more intense for 58 kDa SCP-x and 15.2 kDa pro-SCP-2 expressors as compared to the untransfected L-cells. The cells were examined by conventional epifluorescence microscopy, using an Olympus Vanox AHBS3 photomicroscope; objective, 40×.

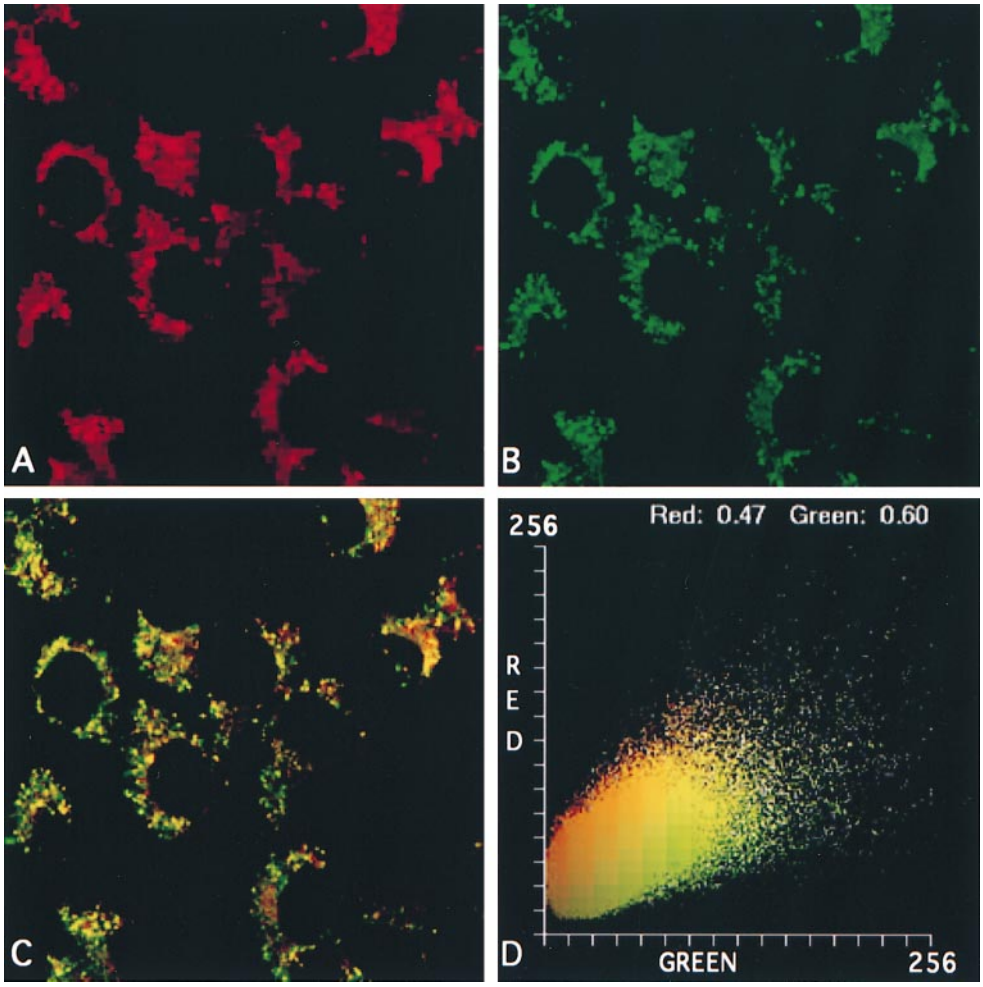

Fig. 7. Double-label immunofluorescence of L-cells transfected with cDNA corresponding to 58 kDa SCP-x. Cells were simultaneously labeled for SCP-x with Texas Red-conjugated goat anti-rabbit IgG (panel A) and catalase with FITC-conjugated donkey anti-sheep IgG (panel B). The punctate pattern obtained with the peroxisomal marker, catalase, was superimposable to that with SCP-x over the same cells (panel C). The superimposition was delineated graphically as a pixel fluorogram (panel D) where colocalization of SCP-x (red) with catalase (green) resulted in yellow to orange points that predominantly fall along the diagonal line in the fluorogram. Points falling outside the diagonal represented non-superimposition. Correlation coefficients representing the extent of co-localization of SCP-x with catalase were 0.47 (red) and 0.6 (green), respectively. Immunostained cells were examined using the Bio-Rad MRC-1024 confocal system; objective, 63×.

mined by culturing the cells with [^{3}H]cholesterol in serum containing medium for various timed intervals. Because the untransfected and the mock transfected cells did not significantly differ from each other in [^{3}H]cholesterol incorporation, they were combined and designated as control. During the first 6 h of [^{3}H]cholesterol uptake, no differences were observed in the 58 kDa SCP-x overexpressing cells versus the control (**Fig. 8**, panel A). However, differences began to be observed between 6–25 h where at 15 h [^{3}H]cholesterol incorporation nearly doubled when compared to the control (**Table 2**, n = 4, $P < 0.002$).

Simply following the distribution of radiolabeled cholesterol in the transfected cells does not allow differentiation of SCP-x expression effects on turnover versus mass increase in free cholesterol. In order to discriminate between the two, it was necessary to determine cholesterol mass by extracting the lipids from the cell lines. Cholesterol mass increased 1.4-fold in the 58 kDa SCP-x expressors (**Table 3**).

Determination of lipid masses at equilibrium allowed calculation of the specific activity of [^{3}H]cholesterol in the cholesterol pool (**Fig. 9**, panel A). [^{3}H]cholesterol incorporation into the free cholesterol pool and the mass of that pool appeared to increase essentially in parallel in the cell lines. As [^{3}H]cholesterol incorporation increased during this time interval but the equilibrium mass values did not (although they were 1.4-fold higher in the expression clones relative to the control), the values appeared to increase but differences between the clones and control were decreased. This was consistent with 58 kDa SCP-x expression increasing the uptake and intracellular mass of extracellular cholesterol rather than increasing the turnover of [^{3}H]cholesterol in the cellular free cholesterol pool.

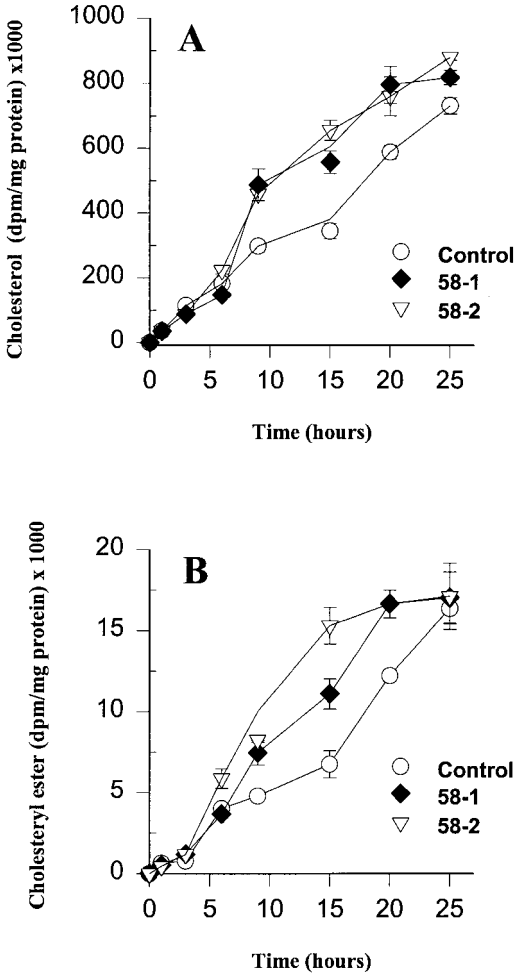

Fig. 8. [^{3}H]cholesterol incorporation and esterification of transfected L-cells. Control and 58 kDa SCP-x expressing cell lines, incubated with [^{3}H]cholesterol for various times, were extracted and resolved into cholesterol (panel A) and cholesteryl ester (panel B) to determine the extent of incorporation and esterification as described in Methods. Data represent mean ± SEM from 3–5 determinations.

Incorporation of [^{3}H]cholesterol into the esterified cholesterol pool of transfected L-cells and [^{3}H]oleic acid esterification into cholesteryl esters

Cellular cholesterol can also be esterified to form cholesteryl esters. As there were no significant differences between the untransfected and mock transfected L-cell data, it was combined and designated as the control. During the first 6 h of [^{3}H]cholesterol uptake, no differences were observed in the appearance of [^{3}H]cholesterol as [^{3}H]cholesteryl esters in the transfected cells versus control cell lines (Fig. 8, panel B). Increased appearance of [^{3}H]cholesteryl esters was observed between 6 and 25 h (Fig. 8, panel B) where [^{3}H]cholesterol esterification was increased maximally up to 2.3-fold (n = 4, $P < 0.005$, Table 2) at 15 h.

TABLE 2. Extent of [^{3}H]cholesterol incorporation and ester formation after 15 h incubation

Lipid	Control	Clone 58-1	Clone 58-2
		pmol/mg protein	
[^{3}H]cholesterol	4.7 ± 0.3	7.7 ± 0.5[a]	9.1 ± 0.4[a]
[^{3}H]cholesteryl ester	0.09 ± 0.01	0.15 ± 0.01[a]	0.21 ± 0.02[a]
Total [^{3}H]cholesterol	4.8 ± 0.3	7.9 ± 0.5[a]	9.3 ± 0.4[a]

Values reflect the mean ± SEM (n = 4); Total cholesterol = [^{3}H]cholesterol + [^{3}H]cholesteryl ester.
[a] $P < 0.005$, significance as compared to control.

TABLE 3. Neutral lipid content of 58 kDa SCP-x expression clones

Lipid Class	Lipid Mass		
	Control	Clone 58-1	Clone 58-2
		μg/mg protein	
Total neutral lipid	70.8 ± 2.3 (4)	88.7 ± 2.2[a] (4)	87.5 ± 2.3[a] (4)
Cholesterol	53.4 ± 1.0 (4)	73.1 ± 0.7[a] (4)	68.2 ± 1.2[a] (4)
Cholesteryl ester	12.7 ± 0.8 (4)	11.2 ± 1.1 (5)	12.7 ± 0.4 (5)
Triglyceride	4.6 ± 0.5 (4)	5.7 ± 0.4 (5)	5.5 ± 0.7 (5)

Values reflect mean ± SEM. The numbers in parentheses indicate the number of experiments performed.
[a] $P < 0.002$, significance as compared to the control cell line.

In order to confirm the enhanced esterification of [^{3}H]cholesterol in the transfected cells, the cells were incubated with [^{3}H]oleic acid. In contrast to the slow uptake of exogenous cholesterol, exogenous free fatty acids are taken up and intracellularly esterified at a much faster rate (22, 52). **Table 4** shows the extent of incorporation after 60 min of incubation where a 2.5- and 2.0-fold increase in cholesterol esterification over the control was observed for clones 58-1 and 58-2, respectively (n = 5–8, $P < 0.0001$). As no significant difference was observed in [^{3}H]oleic acid esterified triglycerides, SCP-x overexpression resulted in selective targeting of fatty acids for esterification to cholesterol rather than triglycerides.

It should be noted that the majority (96–98%) of exogenous [^{3}H]cholesterol (Table 2) was not esterified to cholesteryl esters after 15 h incubation. In order to differentiate between 58 kDa SCP-x expression increased [^{3}H]cholesterol turnover versus mass changes in the cholesterol esters, lipids from the transfected cell lines were extracted and the mass of cholesteryl ester and triglycerides was determined. The equilibrium mass of cholesteryl ester and triglycerides in SCP-x expressors did not significantly differ from L-cell controls (Table 3). Esterification of radiolabeled cholesterol also increased during this interval but now the equilibrium cholesteryl ester mass values were not different from the controls. This led to an increase in specific activity by 1.9- to 2.3-fold in 58 kDa SCP-x expressors (Fig. 9, panel B). Taken together with the lack of cholesteryl ester mass changes, these observations suggest SCP-x overexpression stimulated turnover/cycling of [^{3}H]cholesterol in the cholesteryl ester pool.

DISCUSSION

Although the sterol carrier protein family have been studied for several decades, recent developments in the molecular, structural, and functional arenas have shed new light on the potential physiological role(s) of these ubiquitous proteins. The data presented herein make sev-

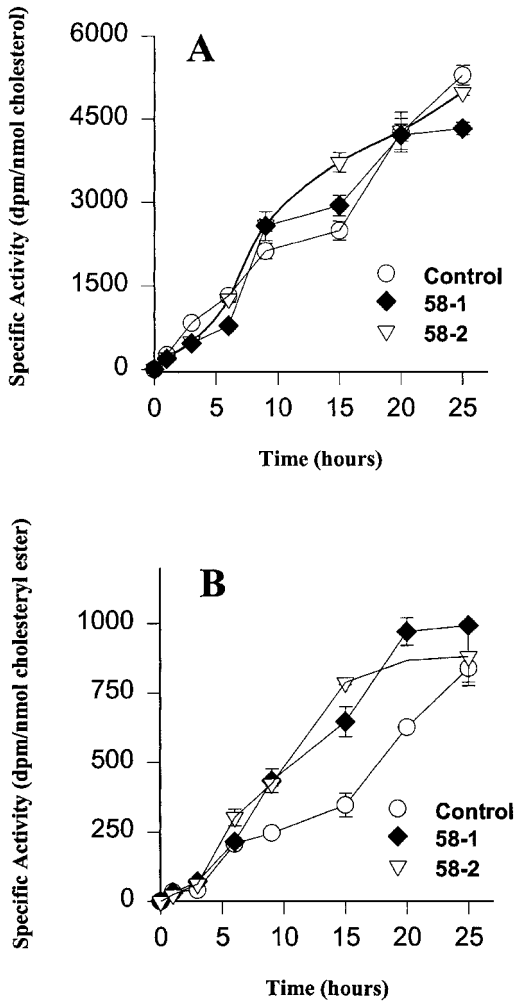

Fig. 9. Specific activity of [^{3}H]cholesterol in cholesterol and cholesteryl ester pools. Experimental data from [^{3}H]cholesterol incorporation and esterification studies was combined with cholesterol and cholesteryl ester mass determinations to give the specific activity (SA) for [^{3}H]cholesterol in cholesterol (panel A) and cholesteryl ester (panel B) pools. Lipids from control and 58 kDa SCP-x expressing cells were extracted and the mass of cholesterol and cholesteryl esters was determined as described in Methods. Data represent mean ± SEM from 3–7 determinations.

TABLE 4. Extent of [^{3}H]oleic acid incorporation into cholesteryl esters and triglycerides

Lipid Class	Control	Clone 58-1	Clone 58-2
		pmol/mg protein	
Triglycerides	5.7 ± 0.5	5.9 ± 0.4	6.0 ± 0.5
Cholesteryl ester	0.4 ± 0.03	1.0 ± 0.05[a]	0.8 ± 0.01[a]

Values represent means ± SEM (n = 5–8).
[a] $P < 0.0001$, significance as compared to control.

eral important contributions to our understanding of the origin of the SCP-2 gene products and of the part they play in cellular cholesterol trafficking.

First, the data suggest that part of the 58 kDa SCP-x protein was processed to the 13.2 kDa SCP-2 in the intact cultured cell system. This conclusion would resolve an important issue regarding the origin of 13.2 kDa SCP-2. Most studies suggest that the 15.2 kDa pro-SCP-2 is processed to the 13.2 kDa SCP-2 form (5–7). However, similar processing of the 58 kDa SCP-x has not previously been demonstrated. In fact, one report even suggested that the 58 kDa SCP-x may not be a precursor of 13.2 kDa SCP-2 (4). However, several findings from this and other laboratories were consistent with the conclusion that not only 15.2 kDa pro-SCP-2, but also the 58 kDa SCP-x, may give rise to the 13.2 kDa SCP-2. *i*) Transfected L-cells expressing SCP-x showed a 2-fold increase in 13.2 kDa SCP-2 protein expression. *ii*) Northern blot analysis on 58 kDa SCP-x mRNA from L-cell clones showed only transcripts corresponding to 58 kDa SCP-x and not the 15.2 kDa pro-SCP-2 protein. *iii*) Antibodies raised against synthetic peptides from the 46 kDa amino terminus of 58 kDa SCP-x cross-reacted with the 58 kDa SCP-x and a 46 kDa thiolase protein from rat liver but not with the smaller 15.2 kDa C-terminus (24, 53). The possibility exists that only one protease is responsible for processing part of the 58 kDa SCP-x and the 15.2 kDa pro-SCP-2 protein, along with one other peroxisomal thiolase. Intracellular targeting and processing of the 58 kDa SCP-x protein is dependent on two peroxisomal targeting signals contained in the C-terminal and N-terminal sites of SCP-x. It has been reported that the N-terminus of SCP-x shares a high degree of homology with 3-oxoacyl-CoA thiolase, a peroxisomal thiolase from rat liver which contains one peroxisomal targeting signal at its N-terminus (46). The pre-sequence of this thiolase contains sequences similar to those near the juncture of the SCP-x thiolase and lipid binding domains (54). Cleavage at this juncture would involve Thr^{424} and Ser^{425} and yield the 13.2 kDa SCP-2 and 46 kDa proteins from SCP-x (54). Thus, it is possible that the protease responsible for generating SCP-2 from SCP-x not only generates SCP-2 from pro-SCP-2, but also is involved in processing 3-oxoacyl-CoA thiolase to the mature form of the protein. These events almost certainly occur inside the peroxisome. Support for this conclusion comes from work involving fibroblasts from patients with rhizomelic chondrodysplasia punctata (RCDP), a disease that affects peroxisomal import and maturation of 3-oxoacyl-CoA thiolase (55). In those studies SCP-2, but not the mature form of 3-oxoacyl-CoA thiolase, was found in peroxisomes isolated from RCDP cells. The pre-thiolase was found in non-peroxisomal fractions. These results indicate that the protease responsible for processing SCP-2 is available in RCDP cells. If this protease is also responsible for pre-thiolase processing then the results suggest that RCDP cells have a defective peroxisomal import machinery for proteins without a second targeting signal at the C-terminus. Furthermore, the results suggest that the proteins are imported into peroxisomes before proteolysis occurs. In summary, the results presented herein taken together with those in the literature are consistent with the 58 kDa SCP-x being processed to the 13.2 kDa SCP-2 protein, with the other cleavage product being the 46 kDa thiolase. However, it must be considered that slower processing (turnover) of the basal level of the 13.2 kDa SCP-2 protein in cells overexpressing

58 kDa SCP-x might also contribute at least in part to higher concentrations of the smaller protein.

Second, putative functions of SCP-x established in vitro must be taken in the context of the intracellular distribution of this protein. For example, while SCP-x stimulates intermembrane lipid transfer in vitro (24), such a function may not necessarily be physiologically relevant if the SCP-x is entirely sequestered in an select organelle which prevents ready access to the other membrane lipid compartments. Double-label immunofluorescence of transfected L-cells overexpressing 58 kDa SCP-x showed significant co-localization of affinity-purified anti-SCP-x immunoreactivity with anti-catalase in peroxisomes. Significant extra-peroxisomal staining was also evident. These findings are supported by immunocytochemical data, both immunogold labeling/electron microscopy and subcellular fractionation, demonstrating that in liver the 58 kDa SCP-x resides nearly exclusively in peroxisomes while the 13.2 kDa SCP-2 has been localized not only in peroxisomes but also extra-peroxisomally (endoplasmic reticulum, mitochondria, and cytosol) (rev. in 48, 50). Peroxisomal proteins such as catalase are synthesized on cytosolic free polyribosomes and are imported as monomers to peroxisomes and assembled into catalytically active tetramers (56). However, under normal conditions very little catalase is detectable outside of peroxisomes. Only in cells from patients with deficient peroxisomal biosynthesis, i.e., Zellweger syndrome, does catalase accumulate in the cytosol due to a peroxisomal import deficiency (57). In L-cells, while some of the non co-localized immunofluorescence could be representative of pre-imported catalase, it is unlikely that over half of the nonsuperimposable signal from anti-SCP-2 is due to non-peroxisomal catalase. This is an important point in view of potential contributions of SCP-2 to cell cholesterol homeostasis. If SCP-2 were exclusively peroxisomal, then it would be difficult to envision a role for SCP-2 in intracellular cholesterol trafficking. However, both immunolocalization and subcellular fractionation data clearly show that SCP-2 gene products are not exclusively peroxisomal in animal tissues (rev. in 48). Neither our work with immunofluorescence in transfected fibroblasts nor that of Van der Krift et al. (49) and Keller et al. (50) using immunogold electron microscopy showed an exclusive localization of SCP-2 gene products in peroxisomes. On the contrary, significant SCP-2 immunoreactivity was extraperoxisomal (endoplasmic reticulum and mitochondria). Further, ongoing work in our laboratory with immunofluorescence co-localization of SCP-2 in other organelles from the L-cell clones has shown that part of the extraperoxisomal signal can be attributed to SCP-2 co-localizing with endoplasmic reticulum and mitochondrial proteins (unpublished data). Furthermore, as peroxisomes account for less than 1% of protein in most cells, even a low level of extra-peroxisomal SCP-2 will quantitatively account for as much as half of total cellular SCP-2 (rev. in 48). In short, the data are entirely consistent with SCP-x having a role in intracellular functions such as cholesterol trafficking as there is an increased presence of 13.2 kDa SCP-2 protein in SCP-x expression cells and, as the immunofluorescence co-localization data show, both peroxisomal and extra-peroxisomal localization of anti-SCP-x immunoreactivity.

Third, there is a close correlation between peroxisomes, cholesterol, and SCP-2 gene products (14, 15, 27, 28, 30, 31). However, prior to the work described herein, there were no reports demonstrating a role for 58 kDa SCP-x expression in cellular cholesterol uptake. The data show for the first time that cellular incorporation of exogenous cholesterol was significantly enhanced by expression of the 58 kDa SCP-x protein in the expression clones (up to 1.9-fold). Total cellular cholesterol and cellular free cholesterol mass were increased 1.3- and 1.4-fold, repectively, at equilibrium. However, additional effects of SCP-2/SCP-x expression may contribute to the increase in cholesterol mass. Cholesterol synthesis might be stimulated in 58 kDa SCP-x expressors. While there is no direct evidence for the 58 kDa SCP-x in this role, the 13.2 kDa SCP-2 protein binds several cholesterol intermediates including geranyl-PP, farnesyl-PP, and dimethylallyl-PP (13) and has been shown to stimulate isopentyl transferase, an enzyme in the cholesterol biosynthetic pathway (14). Also, the SCP-2 gene products may have an indirect effect on fatty acid metabolism. The 13.2 kDa SCP-2 was shown to bind fatty acids (13) and fatty acyl CoAs (58). In the knockout animal, a decrease in serum free fatty acids was observed concomitant with decreased cholesteryl ester and triglycerides in liver (20). Finally, recent data on the sterol regulatory element binding protein provide exciting new links between cholesterol and fatty acid metabolism (59–61).

Fourth, the data established for the first time that 58 kDa SCP-x expression may result in enhanced intracellular turnover/cycling of cholesterol. This effect was observed in the cholesteryl ester, but not free cholesterol, pool. The increase in cell free cholesterol mass could be due either to an expanded cholesterol pool in the plasma membrane which represents 80–90% of cell cholesterol or an increased free cholesterol pool within one or more intracellular compartments. The data on cholesteryl ester turnover suggests that the SCP-x expression affects one or more intracellular compartments, rather than the plasma membrane which is largely devoid of cholesteryl esters. While the cholesteryl esters represented less than 20% of total cholesterol mass, the expression of 58 kDa SCP-x in the transfected L-cells enhanced incorporation of exogenous cholesterol into this fraction. This is consistent with previous data showing that SCP-2 gene products stimulate microsomal acyl CoA cholesteryl acyltransferase in vitro (62–65). Finally, the enhanced esterification to cholesteryl esters appeared specific as [^{3}H] oleic acid esterification to cholesteryl ester was increased 2.5-fold, with no significant change observed in incorporation into triglycerides. However, because the mass of cholesteryl esters and triglycerides was not increased in the 58 kDa SCP-x overexpressing cells, this suggested that the expression of this protein resulted in increased turnover/cycling of the cellular cholesteryl ester pool. This conclusion is supported by other studies in rat hepatoma cells transfected with 15.2 kDa pro-SCP-2 cDNA where a similar increased cycling of cholesterol was observed (7).

While proteolytic processing of some of the 58 kDa SCP-x to 13.2 kDa SCP-2 suggests that the latter protein may be

responsible for the above enhanced cholesterol uptake and intracellular cycling, significant differences exist in effects derived from 13.2 kDa SCP-2 arising from the two SCP-2 gene products. For example, in L-cell clones transfected with cDNA encoding for the 15.2 kDa pro-SCP-2, 13.2 kDa SCP-2 expression was several fold higher than observed in the 58 kDa SCP-x-expressing clones (6). Yet, despite the higher 13.2 kDa SCP-2 expression in the former cell lines, the extent of exogenous cholesterol uptake (6) and esterification (10) was much less (only 1.4- and 1.38-fold, respectively) than observed herein with 58 kDa SCP-x overexpression (1.9- and 2.3-fold, respectively). Results from lipid equilibrium mass determinations also emphasize the differences between the 58 kDa SCP-x and the 15.2 pro-SCP-2 expressors. Results from L-cells transfected with cDNA encoding for the 15 kDa pro-SCP-2 protein showed significantly elevated levels of both cholesterol and cholesteryl ester mass (1.2- and 2-fold, respectively) while triglyceride levels decreased by 60% as compared to the control (6, 10). In contrast, 58 kDa SCP-x expression did not appear to alter the cholesteryl ester or triglyceride mass levels, but cholesterol mass increased 1.4-fold (Table 3). Thus, expression of the 58 kDa SCP-x caused increased changes in the transfected cell's ability to incorporate and esterify cholesterol, changes that differed significantly from those observed in 15.2 kDa pro-SCP-2 expressors.

In summary, the data presented herein are consistent with the intracellular processing of the 58 kDa SCP-x to the 13.2 kDa SCP-2 in transfected L-cell clones expressing 58 kDa SCP-x. Studies with immunofluorescence microscopy showed extensive SCP-2 co-localization with catalase in peroxisomes along with significant extra-peroxisomal staining. Furthermore, the transfected cells showed an enhanced incorporation and esterification of radiolabeled cholesterol suggesting a role for the 58 kDa SCP-x protein in cholesterol trafficking and/or cycling.

This work was supported in part by a grant from the United States Public Health Service, National Institutes of Health (GM-31651, DK-41402). The technical assistance of Amy Boedeker and Andrey Frolov is greatly appreciated.

Manuscript received 30 July 1998 and in revised form 3 November 1998.

REFERENCES

1. Ohba, T., H. Rennert, S. M. Pfeifer, Z. He, R. Yamamoto, J. A. Holt, J. T. Billheimer, and J. F. I. Strauss. 1994. The structure of the human sterol carrier protein X/sterol carrier protein 2 gene (SCP2). *Genomics.* **24:** 370–374.
2. Ohba, T., J. A. Holt, J. T. Billheimer, and J. F. I. Strauss. 1995. Human sterol carrier protein x/sterol carrier protein 2 gene has two promoters. *Biochemistry.* **34:** 10660–10668.
3. Johnson, W. J., and M. P. Reinhart. 1994. Lack of requirement for sterol carrier protein-2 in the intracellular trafficking of lysosomal cholesterol. *J. Lipid Res.* **35:** 563–573.
4. Fujiki, Y., M. Tsuneoka, and Y. Tashiro. 1989. Biosynthesis of nonspecific lipid transfer protein (sterol carrier protein 2) on free polyribosomes as a larger precursor in rat liver. *J. Biochem.* **106:** 1126–1131.
5. Yamamoto, R., C. B. Kallen, G. O. Babalola, H. Rennert, J. T. Billheimer, and J. F. I. Strauss. 1991. Cloning and expression of a cDNA encoding human sterol carrier protein 2. *Proc. Natl. Acad. Sci. USA.* **88:** 463–467.
6. Moncecchi, D. M., E. J. Murphy, D. R. Prows, and F. Schroeder. 1996. Sterol carrier protein-2 expression in mouse L-cell fibroblasts alters cholesterol uptake. *Biochim. Biophys. Acta.* **1302:** 110–116.
7. Baum, C. L., E. J. Reschly, A. K. Gayen, M. E. Groh, and K. Schadick. 1997. Sterol carrier protein-2 overexpression enhances sterol cycling and inhibits cholesterol ester synthesis and high density lipoprotein cholesterol secretion. *J. Biol. Chem.* **272:** 6490–6498.
8. Frolov, A., J. K. Woodford, E. J. Murphy, J. T. Billheimer, and F. Schroeder. 1996. Spontaneous and protein-mediated sterol transfer between intracellular membranes. *J. Biol. Chem.* **271:** 16075–16083.
9. Puglielli, L., A. Rigotti, A. V. Greco, M. J. Santos, and F. Nervi. 1995. Sterol carrier protein-2 is involved in cholesterol transfer from the endoplasmic reticulum to the plasma membrane in human fibroblasts. *J. Biol. Chem.* **270:** 18723–18726.
10. Murphy, E. J., and F. Schroeder. 1997. Sterol carrier protein-2 mediated cholesterol esterification in transfected L-cell fibroblasts. *Biochim. Biophys. Acta.* **1345:** 283–292.
11. Fuchs, M., F. Lammert, D. Q. H. Wang, B. Paigen, M. C. Carey, and D. E. Cohen. 1997. Lith genes induce overexpression of sterol carrier protein 2 during cholesterol gallstone formation. *FASEB J.* **11:** A1060.
12. Ito, T., S. Kawata, Y. Imai, H. Kakimoto, J. Trzaskos, and Y. Matsuzawa. 1996. Hepatic cholesterol metabolism in patients with cholesterol gallstones: enhanced intracellular transport of cholesterol. *Gastroenterology.* **110:** 1619–1627.
13. Frolov, A., K. Miller, J. T. Billheimer, T. C. Cho, and F. Schroeder. 1997. Lipid specificity and location of the sterol carrier protein-2 fatty acid binding site: a fluorescence displacement and energy transfer study. *Lipids.* **32:** 1201–1209.
14. Ericsson, J., T. Scallen, T. Chojnacki, and G. Dallner. 1991. Involvement of sterol carrier protein-2 in dolichol biosynthesis. *J. Biol. Chem.* **266:** 10602–10607.
15. Scallen, T. J., A. Pastuszyn, B. J. Noland, R. Chanderbhan, A. Kharroubi, and G. V. Vahouny. 1985. Sterol carrier and lipid transfer proteins. *Chem. Phys. Lipids.* **38:** 219–261.
16. Chanderbhan, R., A. Kharroubi, B. J. Noland, T. J. Scallen, and G. V. Vahouny. 1986. Sterol carrier protein 2: further evidence for its role in adrenol steroidogenesis. *Endocr. Res.* **12:** 351–370.
17. Vahouny, G. V., R. Chanderbhan, B. Noland, D. Irwin, P. Dennis, J. D. Lambeth, and T. J. Scallen. 1983. Sterol carrier protein. *J. Biol. Chem.* **258:** 11731–11737.
18. McNamara, B. C., and C. R. Jefcoate. 1989. The role of sterol carrier protein 2 in stimulation of steroidogenesis in rat adrena mitochondria by adrenal cytosol. *Arch. Biochem. Biophys.* **275:** 53–62.
19. Chanderbhan, R., T. Tanaka, J. F. Strauss, D. Irwin, B. J. Noland, T. J. Scallen, and G. V. Vahouny. 1983. Evidence for sterol carrier protein-like activity in hepatic, adrenal, and ovarian cytosol. *Biochem. Biophys. Res. Commun.* **117:** 702–708.
20. Seedorf, U., M. Raabe, P. Ellinghaus, F. Kannenberg, M. Fobker, T. Engel, S. Denis, F. Wouters, K. W. A. Wirtz, R. J. A. Wanders, N. Maeda, and G. Assmann. 1998. Defective peroxisomal catabolism of branched fatty acyl coenzyme A in mice lacking the sterol carrier protein-2/sterol carrier protein-x gene function. *Genes Dev.* **12:** 1189–1201.
21. Jolly, C. A., T. Hubbell, W. D. Behnke, and F. Schroeder. 1997. Fatty acid binding protein: stimulation of microsomal phosphatidic acid formation. *Arch. Biochem. Biophys.* **341:** 112–121.
22. Murphy, E. J., D. R. Prows, J. R. Jefferson, and F. Schroeder. 1996. Liver fatty acid binding protein expression in transfected fibroblasts stimulates fatty acid uptake and metabolism. *Biochim. Biophys. Acta.* **1301:** 191–198.
23. Seedorf, U., S. Scheek, T. Engel, C. Steif, H. J. Hinz, and G. Assmann. 1994. Structure-activity studies of human sterol carrier protein 2. *J. Biol. Chem.* **269:** 2613–2618.
24. Seedorf, U., P. Brysch, T. Engel, K. Schrage, and G. Assmann. 1994. Sterol carrier protein X is peroxisomal 3-oxoacyl coenzyme A thiolase with intrinsic sterol carrier and lipid transfer activity. *J. Biol. Chem.* **269:** 21277–21283.
25. Bun-ya, M., M. Maebuchi, T. Kamiryo, T. Kurosawa, M. Sato, M. Tohma, L. L. Jiang, and T. Hashimoto. 1998. Thiolase involved in bile acid formation. *J. Biochem.* **123:** 347–352.
26. Puglielli, L., A. Rigotti, L. Amigo, L. Nunez, A. V. Greco, M. J. Santos, and F. Nervi. 1996. Modulation on introhepatic cholesterol trafficking: evidence by in vivo antisense treatment for the involvement of sterol carrier protein-2 in newly synthesized cholesterol transfer into bile. *Biochem. J.* **317:** 681–687.

27. Liscum, L., and N. K. Dahl. 1992. Intracellular cholesterol transport. *J. Lipid Res.* **33:** 1239–1254.
28. van den Bosch, H., R. B. H. Schutgens, R. J. A. Wanders, and J. M. Tager. 1992. Biochemistry of peroxisomes. *Annu. Rev. Biochem.* **61:** 157–197.
29. Mandel, H., M. Getsis, M. Rosenblat, M. Berant, and M. Aviram. 1996. Impaired cholesterol synthesis rate in fibroblasts and reduced cellular uptake of LDL's derived from peroxisome deficient patients cause cellular cholesterol deficiency in peroxisome deficient fibroblasts. *Ann. NY Acad. Sci.* **804:** 752–755.
30. Krisans, S. K. 1996. Cell compartmentalization of cholesterol biosynthesis. *Ann. NY Acad. Sci.* **804:** 142–164.
31. Appelkvist, E. L., M. Reinhart, R. Fischer, J. T. Billheimer, and G. Dallner. 1990. Presence of individual enzymes of cholesterol biosynthesis in rat liver peroxisomes. *Arch. Biochem. Biophys.* **282:** 318–325.
32. Higuchi, K. 1970. An improved chemically defined culture medium for strain L mouse cells based on growth responses to graded levels of nutrients including iron and zinc. *J. Cell Physiol.* **75:** 65–72.
33. Stern, D. E., and M. Volmer. 1919. Ueber die Ablingungszeit der Fluoreszenz. *Phys. Z.* **20:** 183.
34. Maniatis, T., E. F. Fritsch, and J. Sambrook. 1989. Molecular Cloning. A Laboratory Manual. Cold Spring Harbor Laboratory Press, Cold Spring Harbor, NY.
35. Goldman, L. A., E. C. Cutrone, S. V. Kotenko, C. D. Krause, and J. A. Langer. 1996. Modifications of vectors pEF-BOS, pcDNA1 and pcDNA3 result in improved convenience and expression. *BioTechniques.* **21:** 1013–1015.
36. Lehrach, H., D. Diamond, J. M. Woxney, and H. Boedtker. 1998. RNA molecular weight determinations by gel electrophoresis under denaturing conditions, a critical reexamination. *RNA Molecular Weight Determination*. **16:** 4743–4751.
37. Feinberg, A. P., and B. Vogelstein. 1983. A technique for radiolabeling DNA restriction endonuclease fragments to high specific activity. *Anal. Biochem.* **132:** 6–13.
38. Matsuura, J. E., H. J. George, N. Ramachandran, J. G. Alvarez, J. F. I. Strauss, and J. T. Billheimer. 1993. Expression of the mature and the pro-form of human sterol carrier protein 2 in *Escherichia coli* alters bacterial lipids. *Biochemistry.* **32:** 567–572.
39. Harlow, E. D., and D. Lane. 1988. Antibodies, A Laboratory Manual. E. D. Harlow and D. Lane, editors. Cold Spring Harbor Laboratory Press, Cold Spring Harbor, NY.
40. Pu, L., W. B. Foxworth, A. B. Kier, E. Murphy, W. G. Wood, and F. Schroeder. 1998. Characterization of 30 kDa SCP-2 related protein protein from rat liver. *Protein Exp. Purif.* **13:** 337–348.
41. Bradford, M. 1976. A rapid and sensitive method for the quantitation of microgram quantities of protein utilizing the principle of protein dye-binding. *Anal. Biochem.* **72:** 248–254.
42. Jefferson, J. R., J. P. Slotte, G. Nemecz, A. Pastuszyn, T. J. Scallen, and F. Schroeder. 1991. Intracellular sterol distribution in transfected mouse L-cell fibroblasts expressing rat liver fatty acid binding protein. *J. Biol. Chem.* **266:** 5486–5496.
43. Hara, A., and N. S. Radin. 1978. Lipid extraction of tissues with a low toxicity solvent. *Anal. Biochem.* **90:** 420–426.
44. Marzo, A., P. Ghirardi, D. Sardini, and G. Meroni. 1971. Simplified measurement of monoglycerides, diglycerides, triglycerides, and free fatty acids in biological samples. *Clin. Chem.* **17:** 145–147.
45. Moncecchi, D. M., A. Pastuszyn, and T. J. Scallen. 1991. cDNA sequence and bacterial expression of mouse liver sterol carrier protein-2. *J. Biol. Chem.* **266:** 9885–9892.
46. Mori, T., T. Tsukamoto, H. Mori, Y. Tashiro, and Y. Fujiki. 1991. Molecular cloning and deduced amino acid sequence of nonspecific lipid transfer protein (sterol carrier protein 2) of rat liver: a higher molecular mass (60 kDa) protein contains the primary sequence of nonspecific lipid transfer protein as its C-terminal part. *Proc. Natl. Acad. Sci. USA.* **88:** 4338–4342.
47. Seedorf, U., U. Raabe, and G. Assmann. 1993. Cloning, expression and sequence of SCP-X encoding cDNAs and a related pseudogene. *Gene.* **123:** 165–172.
48. Schroeder, F., A. Frolov, J. Schoer, A. Gallegos, B. P. Atshaves, N. J. Stolowich, A. I. Scott, and A. B. Kier. 1998. Intracellular sterol binding proteins, cholesterol transport and membrane domains. *In* Intracellular Cholesterol Trafficking. T. Y. Chang and D. E. Freeman, editors. Kluwer Press, Boston, MA. 213–234.
49. Van der Krift, T. P., J. Leunissen, T. Teerlink, G. P. H. van Heusden, A. J. Verklij, and K. W. A. Wirtz. 1985. Ultrastructural localization of a peroxisomal protein in rat liver using the specific antibody against the nonspecific lipid transfer protein (sterol carrier protein-2). *Biochim. Biophys. Acta.* **812:** 387–392.
50. Keller, G. A., T. J. Scallen, D. Clarke, P. A. Maher, S. K. Krisans, and S. J. Singer. 1989. Subcellular localization of sterol carrier protein-2 in rat hepatocytes: its primary localization to peroxisomes. *J. Cell Biol.* **108:** 1353–1361.
51. Demandolx, D., and J. Davoust. 1997. Multicolour analysis and local image correlation in confocal microscopy. *J. Microsc.* **185:** 21–36.
52. Heyliger, C. E., T. J. Kheshgi, E. J. Murphy, S. Myers-Payne, and F. Schroeder. 1996. Fatty acid double orientation alters interaction with L-cell fibroblasts. *Mol. Cell. Biochem.* **155:** 113–119.
53. Ossendorp, B. C., W. F. Voorhout, A. Van Amerongen, F. Brunink, J. J. Batenburg, and K. W. A. Wirtz. 1996. Tissue-specific distribution of a peroxisomal 46-kDa protein related to the 58-kDa protein (sterol carrier protein X; sterol carrier protein 2/3-oxoacyl-CoA thiolase). *Arch. Biochem. Biophys.* **334:** 251–260.
54. Seedorf, U., T. Engel, G. Assmann, F. Leenders, and J. Adamski. 1995. Intrinsic sterol- and phosphatidylcholine transfer activities of 17 beta-hydroxysteroid dehydrogenase type IV. *J. Steroid Biochem. Mol. Biol.* **55:** 549–553.
55. Heikoop, J. C., B. C. Ossendorp, R. J. Wanders, K. W. Wirtz, and J. M. Tager. 1992. Subcellular localization and processing of nonspecific lipid transfer protein are not aberrant in rhizomelic chondrodysplasia punctata fibroblasts. *FEBS Lett.* **299:** 201–204.
56. Purdue, P. E., and P. B. Lazarow. 1996. Targeting of human catalase to peroxisomes is dependent upon a novel COOH-terminal perosixomal targeting sequence. *J. Cell. Biol.* **134:** 849–862.
57. Singh, I., K. Kremser, B. Ghosh, A. Singh, and S. Pai. 1996. Abnormality in translational regulation of catalase expression in disorders of peroxisomal biogenesis. *J. Neurochem.* **67:** 2373–2378.
58. Frolov, A., T. H. Cho, J. T. Billheimer, and F. Schroeder. 1996. Sterol carrier protein-2, a new fatty acyl coenzyme A-binding protein. *J. Biol. Chem.* **271:** 31878–31884.
59. Worgall, T. S., S. L. Sturley, T. Seo, T. F. Osborne, and R. J. Deckelbaum. 1998. Polyunsaturated fatty acids decrease expression of promoters with sterol regulatory elements by decreasing levels of mature sterol regulatory element-binding protein. *J. Biol. Chem.* **273:** 25537–25540.
60. Horton, J. D., I. Shimomura, M. S. Brown, R. E. Hammer, J. L. Goldstein, and H. Shimano. 1998. Activation of cholesterol synthesis in preference to fatty acid synthesis in liver and adipose tissue of transgenic mice overproducing sterol regulatory element-binding protein-2. *J. Clin. Invest.* **101:** 2331–2339.
61. Brown, M. S., and J. L. Goldstein. 1998. Sterol regulatory element binding proteins (SREBPs): controllers of lipid synthesis and cellular uptake. *Nutr. Rev.* **56:** S54–S75.
62. Schroeder, F., P. Butko, G. Nemecz, and T. J. Scallen. 1990. Interaction of fluorescent delta 5,7,9(11),22-ergostatetraen-3-ol with sterol carrier protein-2. *J. Biol. Chem.* **265:** 151–157.
63. Poorthuis, B. J. H. M., and K. W. A. Wirtz. 1982. Increased cholesterol esterification in rat liver microsomes by purified nonspecific phospholipid transfer protein. *Biochim. Biophys. Acta.* **710:** 99–105.
64. Trzaskos, J. M., and J. L. Gaylor. 1983. Cytosolic modulators of activities of microsomal enzymes of cholesterol biosynthesis. Purification and characterization of a non-specific lipid-transfer protein. *Biochim. Biophys. Acta.* **751:** 52–65.
65. van Haren, L., K. J. Teerds, B. C. Ossendorp, G. P. H. van Heusden, J. Orly, D. M. Stocco, K. W. A. Wirtz, and F. F. G. Rommerts. 1992. Sterol carrier protein 2 (non-specific lipid transfer protein) is localized in membranous fractions of Leydig cells and Sertoli cells but not in germ cells. *Biochim. Biophys. Acta.* **1124:** 288–296.